Catalysis Communications 10 (2009) 1656–1660

Contents lists available at ScienceDirect

Catalysis Communications

journal homepage: www.elsevier.com/locate/catcom

Nickel catalysts applied in steam reforming of glycerol for hydrogen production

Ivana N. Buffoni, Francisco Pompeo, Gerardo F. Santori, Nora N. Nichio *

Facultad de Ingeniería, Universidad Nacional de La Plata, 1 esq. 47, 1900 La Plata, Argentina
CINDECA, Facultad de Ciencias Exactas, Universidad Nacional de La Plata-CONICET, 47 N° 257, 1900 La Plata, Argentina

ARTICLE INFO

Article history:
Received 26 February 2009
Received in revised form 4 May 2009
Accepted 6 May 2009
Available online 12 May 2009

Keywords:
Glycerol
Steam reforming
Hydrogen
Supported nickel

ABSTRACT

In order to study catalysts to obtain hydrogen by steam reforming of glycerol, nickel catalysts supported on commercial α-Al_2O_3 and α-Al_2O_3 modified by addition of ZrO_2 and CeO_2 were prepared and characterized. Results show the support effect on stability of catalysts in this reaction carried out at atmospheric pressure and in the range 450–600 °C. The most stable system resulted to be Ni/CeO_2/α-Al_2O_3. Results can be explained due to the Ce effect in inhibition of secondary dehydration reactions forming unsaturated hydrocarbons that are coke precursors generating fast catalyst deactivation.

1. Introduction

Due to the need of alternative energies, biomass resources appear as raw materials available for providing new energy sources and chemical intermediates. For this reason, several processes of biomass conversion are being developed in chemical specialties (methanol), light alkanes (C_1–C_6), liquid fuels (ethanol and alkanes C_7–C_{15}) and syngas (H_2 and CO) [1].

As a new alternative, glycerol can be converted catalytically in a gaseous mixture of H_2 and CO (syngas), which can be used to produce fuels and chemicals [2,3].

A glycerol source for these purposes is the by-product of transesterification of vegetable oils and animal fats generated in biodiesel production. This waste glycerol stream has low commercial value; it contains glycerol in water with an approximate concentration 80% w/w. However, this is not the only source since glycerol can come from sugar fermentation, in direct form or as by-product of ethanol production by lignocellulose conversion.

From bibliography, it has been reported that catalysts based on transition metals used in methane steam reforming result to be active for glycerol reforming [4]. It is important to consider, due to the important differences in costs, the design and development of catalysts based on Ni. Nevertheless, the most important difficulties presented by the Ni catalysts are the high carbon formation rate.

In previous studies performed to improve the catalytic stability of nickel, we have proposed different modifications in catalyst formulation. Among them, the Sn addition, where the lower carbon deposition is explained considering that carbon formation reactions are more sensitive to the structure than the formation reactions of syngas [5]. Other alternative applied was the use of supports modified by addition of alkaline metals as Li or K [6]. Referring to supports, α-Al_2O_3 is characterized by the stability in its crystalline structure, high availability and low cost. However, it presents the disadvantage of its low reactivity and surface area affecting the metallic dispersion and the metal-support interaction.

On the other hand, advantages of using supports as ZrO_2 and CeO_2 have been demonstrated since they improve the metallic dispersion, they decrease the sintering, they improve the thermal stability and improve the oxygen storage capacity, and this property helps carbon gasification [7–9].

In the present work, the objective is to study the effect of the addition of ZrO_2 and CeO_2 oxides on a commercial α-Al_2O_3 support, on the activity and stability of Ni catalysts with respect to the steam reforming reaction of glycerol.

2. Experimental

Commercial α-Al_2O_3 Rhone Poulenc (Spheralite 512; surface area around 10 $m^2\ g^{-1}$) was used as base support. Modified supports were prepared by impregnations of α-Al_2O_3 with $ZrO(NO_3)_2xH_2O$ (Aldrich) or $Ce(NO_3)_36H_2O$ (Alpha) aqueous solutions. The modified supports with 5% w/w of ZrO_2 or CeO_2, are designated as Zrα and Ceα, respectively. The Ni impregnation was carried out with a $Ni(NO_3)_36H_2O$ (Aldrich) aqueous solution to reach a final metallic content of 2% w/w. After drying at 120 °C for 12 h the samples were calcined in air flow at 750 °C for 4 h [10].

* Corresponding author. Tel./fax: +54 221 4254277.
E-mail address: nnichio@quimica.unlp.edu.ar (N.N. Nichio).

1566-7367/$ - see front matter © 2009 Elsevier B.V. All rights reserved.
doi:10.1016/j.catcom.2009.05.003

X-ray diffraction spectra were obtained in an equipment Philips PW 1740 X-ray diffractometer with CuKα radiation in the range 2Theta = 20–80° with scanning rate 0.028° min^{-1}. Acid–base properties of supports were determined by an indirect method that is the reaction test of isopropanol decomposition (IPA). This reaction was tested in a fixed bed continuous flow reactor between 150 and 400 °C, atmospheric pressure, feed 4.5% IPA in helium with flow 40 cm^3 min^{-1} (measured at room temperature and pressure).

Temperature programmed reduction tests (TPR) were carried out in a conventional dynamic equipment with H_2/N_2 ratio in the feed of 1/9 and the heating rate 10 °C min^{-1} from room temperature up to 1000 °C.

Measurements of mean particle size determined by TEM were obtained in an equipment TEM JEOL 100 C operated at 200 KV. To estimate the average particle size, the particles were considered spherical and the diameter volume–area was calculated by using the following expression: $d_{va} = \frac{\sum ni \cdot di^3}{\sum ni \cdot di^2}$, where ni is the number of particles with diameter *di* [11].

Hydrogen chemisorption measurements were carried out in a dynamic equipment with a TCD detector. Samples were reduced in H_2 at 700 °C for 1 h, cooled in hydrogen up to 400 °C, flushed with argon for 2 h at 400 °C and then cooled up to room temperature in argon flow. Hydrogen pulses were then injected up to saturation. Dispersions were estimated from the hydrogen amount consumed, assuming an adsorption stoichiometry H/Ni = 1.

The experimental equipment used for reaction tests is a quartz fixed bed reactor (8 mm internal diameter) isothermally operated at atmospheric pressure. The catalyst sample (200 mg with particle size 0.12–0.15 mm) was previously reduced to 600 °C in H_2 pure flow (30 cm^3 min^{-1}, at room temperature and pressure) for 2 h.

The aqueous solution of glycerol (molar ratio H_2O/glycerol = 6) was injected to the reactor by a HPLC pump (Waters 590) with feed flow 0.022 cm^3 min^{-1}. Nitrogen was used as carrier gas. To vaporize the reacting mixture, this one is injected in the upper zone packed with quartz balls. The products leaving the reactor were condensed and separated into liquid and gaseous fractions. The outlet products were analyzed on line by gas chromatography, using a packed column HayeSep D 110-120. Products of liquid phase were identified by CG/MS (Shimadzu GCMS-QP5050A) with capillary column SPB-5TM (Supelco).

The glycerol conversion and the selectivity to different reaction products were calculated based on Reactions (1)–(4):

$$\text{Glycerol decomposition}: C_3H_8O_3 \overset{H_2O}{\leftrightarrow} 3CO + 4H_2 \quad (1)$$

$$\text{Water—Gas shift reaction}: CO + H_2O \leftrightarrow CO_2 + H_2 \quad (2)$$

$$\text{Steam reforming of glycerol}: C_3H_8O_3 + 3H_2O \leftrightarrow 3CO_2 + 7H_2 \quad (3)$$

$$\text{Methanation reaction}: CO + 3H_2O \leftrightarrow CH_4 + H_2O. \quad (4)$$

The glycerol conversion to gaseous products (CO, H_2, CO_2 and CH_4) is indicated as X_G% and it was calculated based on the following equation:

$$X_G\% = \frac{\text{C moles in gas products}}{3 \times \text{glycerol moles in the feedstock}} \times 100.$$

The distribution of products indicated as H_2, CO, CO_2 and CH_4% mol/mol was calculated as: produced moles of H_2, CO, CO_2 and CH_4, respectively, divided total moles of gas phase × 100.

The H_2 yield% was calculated based on the following equation:

$$H_2 \text{ yield}\% = \frac{H_2 \text{ moles produced}}{\text{glycerol moles in the feedstock}} \times \frac{100}{7}.$$

where 7 is the maximum number of H_2 moles that can be produced per glycerol mole, according to Eq. (3). Carbon deposits were characterized by temperature programmed oxidation (TPO), in a thermogravimetric equipment (Shimadzu TGA50). Post-reaction samples of 0.015 g were used, air feed flow of 40 cm^3 min^{-1} (at room temperature and pressure), and a heating program of 10° min^{-1} from room temperature up to 850 °C.

3. Results and discussion

3.1. Catalyst characterization

With respect to textural properties of supports, aluminas modified by CeO_2 and ZrO_2 have a BET area of about 7 m^2 g^{-1}, lower than 10 m^2 g^{-1} of commercial α-Al_2O_3.

Table 1 reports isopropanol conversion results (X_{IPA}) and selectivity to acetone (S_A) and propylene (S_P) obtained in the isopropanol decomposition reaction at 300 °C, which allows to determine qualitative differences in surface acid–base properties of supports [12].

It is possible to observe that the presence of alumina modifier oxides increases the global activity of isopropanol decomposition due to the increase of surface active sites. Also, a higher selectivity to acetone is noticed, which indicates that the isopropanol dehydrogenation reaction is favored with respect to pure alumina. This would indicate the presence of larger number of basic sites in Ceα support.

Characterization of supports by XRD allowed distinguishing the presence of peaks characteristic of modifier oxides. Fig. 1 shows, for Ceα support, the most intense peaks corresponding to cubic CeO_2 (PCPDFWIN 81-0792) at 2Theta = 28.54° (*) and 47.47° (▲) and for Zrα, peaks of higher intensity corresponding to the tetragonal phase of ZrO_2 (PCPDFWIN 88-1007) at 2Theta = 30.27° (○) and 50.36° (◘).

With respect to catalysts, H_2 chemisorption results by pulses are shown in Table 2. The Niα system presents a metallic dispersion

Table 1
Results of isopropanol decomposition reaction at 300 °C. X_{IPA} (%): isopropanol conversion, S_A (%): selectivity to acetone and S_P (%): selectivity to propylene.

Support	X_{IPA} (%)	S_A (%)	S_P (%)
α	21	3	97
Zrα	23	9	91
Ceα	30	12	88

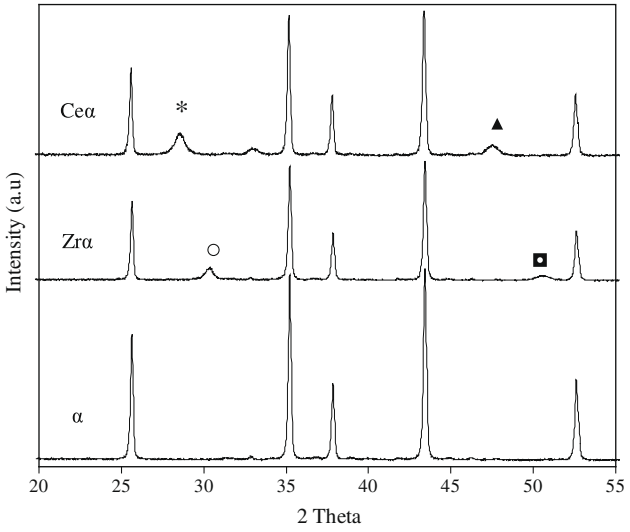

Fig. 1. XRD diffraction patterns for α, Ceα and Zrα supports in the region 2Theta = 20–55°. (*) and (▲) correspond to cubic CeO_2 from PCPDFWIN 81-0792. (○) and (◘) correspond to tetragonal ZrO_2 from PCPDFWIN 88-1007.

Table 2
Characterization of the studied catalysts. Ni dispersions, mean particle size (d_{va}) and metallic surface area calculated by TEM and H_2 chemisorption.

Catalyst	TEM			H_2 chemisorption	
	Average particle diameter d_{va}* (nm)	Dispersion** (%)	Surface area (m^2/g)	Dispersion (%)	Surface area (m^2/g)
Niα	18	4.84	0.64	2.3	0.31
NiZrα	16	5.45	0.77	5.4	0.74
NiCeα	14	6.23	0.84	5.6	0.77

* $d_{va} = \frac{\sum ni \cdot di^3}{\sum ni \cdot di^2}$, ni is the number of particles with diameter di.
** Dispersion $= \frac{(10n^2+2n+1)}{(4n^3+6n^2+3n+1)}$, where $n = \frac{d_{va}}{a}$ (a = Nickel cell-edge length (0.348 nm)), see Ref. [11].

around 2%, noticing that with the support modification, it increases to 5% for NiCeα and NiZrα. These dispersion results are in agreement with average sizes of particles obtained by TEM, for NiCeα and NiZrα are about 14 and 16 nm, respectively, while for Niα is 18 nm.

Fig. 2 shows TPR profiles of catalysts studied. The Niα catalyst presents three principal peaks at 463, 555 and 835 °C, corresponding to: (i) NiO bulk of very weak interaction with the support, (ii) mixed oxide of nickel and aluminum with fairly strong interaction with the support and (iii) $NiAl_2O_4$ species of very strong interaction with the support [13]. In catalysts with modified supports, the intensity decrease of the signal at low temperature (≈450 °C) would indicate a decrease of the NiO bulk weakly interacting, whereas the increase of hydrogen consumption peaks at higher temperature could be related to NiO_x species strongly interacting with CeO_2 and ZrO_2 of the support. It is clear that with the decrease of NiO bulk and with the appearance of Ni^{+2} species that reduce at higher temperatures, the interaction metal-support increases, and as we have reported in a previous work, this improves the resistance of the active phase to sintering [14].

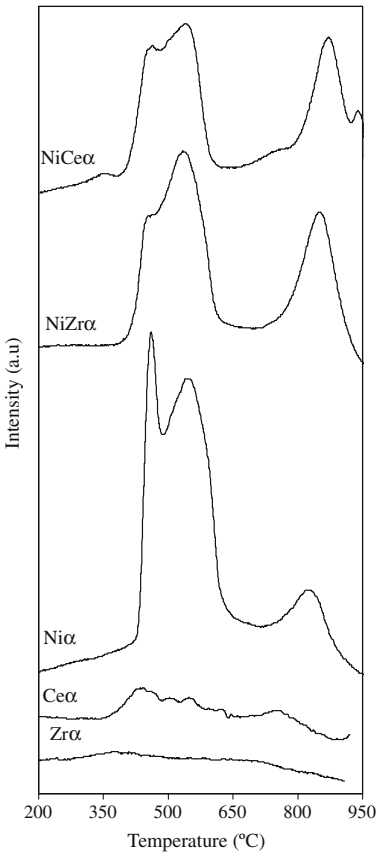

Fig. 2. Temperature programmed reduction (TPR) profiles for Niα, NiCeα, NiZrα catalysts and Ceα, Zrα supports.

3.2. Reaction test

Respect to the reaction of steam reforming of glycerol, thermodynamic studies predict that high temperatures, low pressures and high H_2O/C ratio favor hydrogen production. According to Adhikari et al. [15,16], the better condition to obtain hydrogen is at temperatures higher than 627 °C with a 9:1 molar ratio of water to glycerol. Under these conditions, methane production is minimized and carbon formation is thermodynamically inhibited. Although excess water allows higher selectivity to hydrogen, a significant water amount in reaction products is not beneficial. Thus, in this work, reaction tests were carried out in a temperature range from 450 to 600 °C, water–glycerol molar ratio: 6/1 and gas hourly space velocity (GHSV): 3.9×10^4 cm^3 h^{-1} g_{cat}^{-1}.

Results of reaction tests at temperatures lower than 450 °C showed low conversion levels to gaseous products, $X_G < 40\%$, H_2 yield ≈ 20%, and methane content $CH_4 \approx 15\%$ mol/mol in gaseous reaction products. Condensed reaction products presented a yellowish color and by gas chromatography CG/MS unsaturated compounds were identified (not quantified) such as 1-hydroxy-2-propanone, acetic acid, 1-2 propane diol, propanol and 2-methyl-2-cyclopentenone. A fast deactivation was observed in first reaction hour together with the increase of pressure drop in the reactor.

On the contrary, from 450 °C, total glycerol conversion to gaseous products was reached, with high H_2 content (>59% mol/mol) and CO_2 as principal carbonated product (>18% mol/mol). Table 3 shows activity results after 1 h reaction. Since the distribution of products does not vary considerably with the catalyst, in this table the reaction temperature effect is shown for NiCeα. It is possible to observe that when the temperature increases, the H_2 content increases from 59 to 70% mol/mol (corresponding to yield H_2% 84–100%), while there is a decrease of CO (from 16 to 10% mol/mol) and CH_4 (from 3 to 0.5% mol/mol).

We can explain our results taking into account the reaction way proposed by other researchers in the literature. For the cleavage of C–C or C–O bonds of glycerol molecule, it is necessary a first dehydrogenation step on the metal surface to give adsorbed intermediates [17–19]. In nickel catalysts, the strong capacity for breaking the C–C bond would lead to formation of CO and H_2. From thermodynamic considerations, at low temperatures, the steam reforming reaction is limited due to its endothermy. Meanwhile, water–gas shift and methanation reactions (Eqs. (2) and (4)) are favored by low temperatures. Our results would indicate that when the reaction temperature increases, the contribution of the steam reforming reaction is higher than the glycerol decomposition reaction. In the same way, the methane decrease could be explained by the lower contribution of the methanation reaction at higher temperatures.

At low temperatures (<450 °C), the capacity to break C–C bonds is lower, allowing that dehydrogenated intermediates suffer dehy-

Table 3
Gaseous product distribution in the steam reforming of glycerol over nickel catalysts after 1 h reaction.

Sample	T (°C)	Gas product composition [% mol/mol (dry basis)]				H_2/CO_2	C deposited* (TPO/TGA)
		H_2	CO	CO_2	CH_4	mol/mol	% w/w
NiCeα	450	59.04	16.44	21.41	3.11	2.7	n.d.
NiCeα	550	67.01	10.88	20.98	1.13	3.2	n.d.
NiCeα	600	70.57	10.03	18.91	0.49	3.7	17
NiZrα	600	71.07	9.94	17.89	1.10	3.9	23
Niα	600	69.90	8.86	19.65	1.59	3.5	39

* Carbon content (% w/w) in the Niα, NiZrα and NiCeα catalysts after 10 h of steam reforming reaction at 600 °C.

dration reactions, rearrangement and condensation. These secondary reactions result favored by the presence of support acid sites and would lead to the appearance of products identified in liquid phase (unsaturated compounds). These products represent a group of intermediate products of coke formation, which would explain the fast activity fall and strong increase of pressure drop in the reactor.

The most significant differences among catalysts studied were observed in the catalytic stability. Systems result more stable at high temperature than at low temperatures in agreement with the higher conversion to liquid products determined at low temperatures.

In stability tests at 600 °C, the selected GHSV (3.9×10^4 cm^3 h^{-1} g_{cat}^{-1}) allows to obtain total glycerol conversion to gaseous products without oversize of the catalytic bed that can mask deactivation. Fig. 3a and b show that the Niα catalyst reached values of X_G: 56% and H_2 yield: 33.6% at 8 h reaction, so the system resulted less stable. The NiZrα catalyst resulted more stable with X_G: 64% and H_2 yield: 42% at 11 h reaction. The most stable system resulted to be NiCeα with X_G: 90% and H_2 yield: 86% at 11 h reaction.

Results of TPO/TGA analyses of post-stability test samples indicated that Niα and NiZrα samples presented a higher carbon content 39 and 23% w/w, respectively, while in NiCeα system was 17% w/w (Table 3). Due to the correlation between the lower content of carbon deposits and the higher stability, we can estimate that the preponderant deactivation mechanism is the coke formation.

In this way, the most basic character of Ceα support, if compared with Zrα or α, decreases dehydration reactions of adsorbed dehydrogenated fragments and consequently, unsaturated compounds decrease. Thus, the production of coke precursors or intermediate compounds is lower with Ceα support.

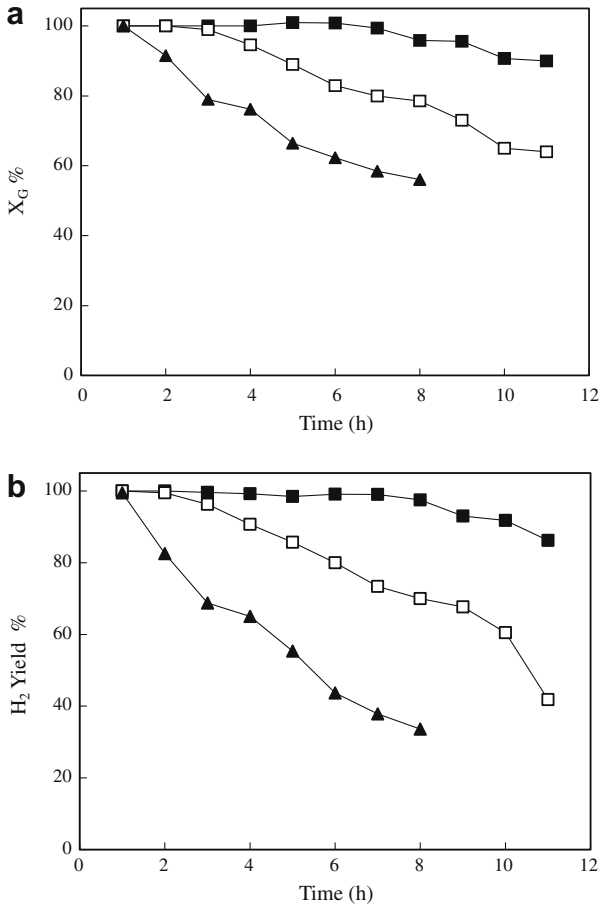

Fig. 3. Stability tests at 600 °C of the studied catalysts. (▲) Niα (□) NiZrα and (■) NiCeα. (a) Glycerol conversion X_G% as a function of time on stream. (b) H_2 yield% as a function of time on stream.

4. Conclusions

The present study indicates that the nickel catalysts resulted to be active and selective with strong dependence on the reaction temperature with glycerol conversion to gaseous products. This indicated that 550 °C is the minimum temperature required to obtain hydrogen with high selectivity.

The support effect is evidenced in stability evaluation. The NiCeα catalyst presented the lower coke formation and higher stability. The highest basic character of NiCeα would inhibit lateral dehydration, rearrangement and condensation reactions that lead to intermediate compounds in the coke formation.

Acknowledgments

The present work has been financed by CONICET (PIP 02738) and ANPCYT–FONCYT (14-14122), Argentina.

References

[1] G.W. Huber, S. Iborra, A. Corma, Chem. Rev. 106 (2006) 4044.
[2] M. Slinn, K. Kendall, C. Mallon, J. Andrews, Bioresource Technology 99 (2008) 5851.
[3] R.R. Soares, D.A. Simonetti, J.A. Dumesic, Angew. Chem. Int. Ed. 45 (2006) 3982.
[4] T. Hirai, N. Ikenaga, T. Miyake, T. Suzuki, Energy and Fuels 19 (2005) 1761.
[5] N.N. Nichio, M.L. Casella, G.F. Santori, E.N. Ponzi, O.A. Ferretti, Catalysis Today 62 (2000) 231.
[6] F. Pompeo, N.N. Nichio, M.G. González, M. Montes, Catalysis Today 107–108 (2005) 856.
[7] J.W.C. Liberatori, R.U. Ribeiro, D. Zanchet, F.B. Noronha, J.M.C. Bueno, Applied Catalysis A General 327 (2007) 197.
[8] F. Dong, A. Suda, T. Tanabe, Y. Nagai, H. Sobukawa, H. Shinjoh, M. Sugiura, C. Descorme, D. Duprez, Catalysis Today 90 (2004) 223.
[9] G. Dutta, U.V. Waghmare, T. Baidya, M.S. Hegde, K.R. Priolkar, P.R. Sarode, Catalysis Letters 108 (2006) 165.
[10] F. Pompeo, D. Gazzoli, N.N. Nichio, Materials Letters 63 (2009) 477.
[11] J.P. Brunelle, A. Sugier, J.F. Le Page, Journal of Catalysis 43 (1976) 273.

[12] A. Gervasini, J. Fenyvesi, A. Auroux, Catalysis Letters 43 (1997) 219.
[13] R. Molina, G. Poncelet, Journal of Catalysis 173 (1998) 257.
[14] F. Pompeo, D. Gazzoli, N.N. Nichio, International Journal of Hydrogen Energy 34 (2009) 2260.
[15] S. Adhikari, S. Fernando, A. Haryanto, Energy and Fuels 21 (2007) 2306.
[16] S. Adhikari, S. Fernando, S.R. Gwaltney, S.D. Filip To, R. Marck Bricka, Philip H. Steele, A. Haryanto, International Journal of Hydrogen Energy 32 (2007) 2875.
[17] R.D. Cortright, R.R. Davda, J.A. Dumesic, Nature 418 (2002) 964.
[18] B. Zhang, X. Tang, Y. Li, Y. Xu, W. Shen, International Journal of Hydrogen Energy 32 (2007) 2367.
[19] S. Adhikari, S. Fernando, A. Haryanto, Renewable Energy 33 (2008) 1097.